BIOCHEMISTRY
including biophysical chemistry & molecular biology

Article

pubs.acs.org/biochemistry

Temperature Invariance of the Nitrogenase Electron Transfer Mechanism

Diana Mayweather,[†] Karamatullah Danyal,[‡] Dennis R. Dean,[§] Lance C. Seefeldt,*[,‡] and Brian M. Hoffman*[,†]

[†]Department of Chemistry, Northwestern University, Evanston, Illinois 60208, United States

[‡]Department of Chemistry and Biochemistry, Utah State University, Logan, Utah 84322, United States

[§]Department of Biochemistry, Virginia Tech University, Blacksburg, Virginia 24061, United States

Supporting Information

ABSTRACT: Earlier studies of electron transfer (ET) from the nitrogenase Fe protein to the MoFe protein concluded that the mechanism for ET changed during cooling from 25 to 5 °C, based on the observation that the rate constant for Fe protein to MoFe protein ET decreases strongly, with a nonlinear Arrhenius plot. They further indicated that the ET was reversible, with complete ET at ambient temperature but with an equilibrium constant near unity at 5 °C. These studies were conducted with buffers having a strong temperature coefficient. We have examined the temperature variation in the kinetics of oxidation of the Fe protein by the MoFe protein at a constant pH of 7.4 fixed by the buffer 3-(*N*-morpholino)propanesulfonic acid (MOPS), which has a very small temperature coefficient. Using MOPS, we also observe temperature-dependent ET rate constants, with nonlinear Arrhenius plots, but we find that ET is gated across the temperature range by a conformational change that involves the binding of numerous water molecules, consistent with an unchanging ET mechanism. Furthermore, there is no solvent kinetic isotope effect throughout the temperature range studied, again consistent with an unchanging mechanism. In addition, the nonlinear Arrhenius plots are explained by the change in heat capacity caused by the binding of waters in an invariant gating ET mechanism. Together, these observations contradict the idea of a change in ET mechanism with cooling. Finally, the extent of ET at constant pH does not change significantly with temperature, in contrast to the previously proposed change in ET equilibrium.

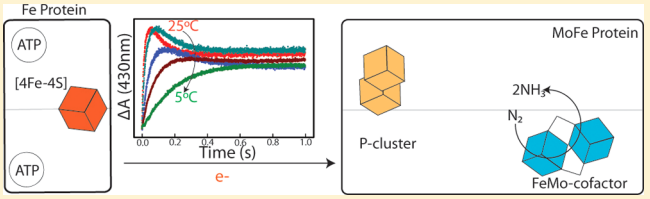

Nitrogenase catalyzes the multielectron reduction of dinitrogen (N_2) to ammonia (NH_3), a reaction that is the major pathway for N_2 fixation in the biosphere.[1] The enzyme comprises two component proteins, called the Fe protein and the MoFe protein, which associate and dissociate each time an electron is delivered from the Fe protein to the MoFe protein, which contains the catalytically active FeMo cofactor, [7Fe,Mo,9S;C;homocitrate].[2−4] This process of electron transfer (ET) from Fe to MoFe protein can be summarized by the deceptively simple kinetic scheme of eq 1. The reduced Fe protein with two bound molecules of ATP [$Fe^{red}(MgATP)_2$] rapidly forms an activated complex with the MoFe protein, where the rate constant for binding is k_1 and that for dissociation is k_{-1}

$$\begin{aligned} &Fe^{red}(MgATP)_2 + MoFe \\ &\underset{k_{-1}}{\overset{k_1}{\leftrightarrow}} [Fe^{red}(MgATP)_2;MoFe]^* \\ &\underset{k_{-2}}{\overset{k_2}{\leftrightarrow}} [Fe^{ox}(MgAXP)_2:MoFe^{red}] \end{aligned} \quad (1)$$

ET from the Fe protein to the MoFe protein then creates a one-electron reduced MoFe protein denoted $MoFe^{red}$. This forward ET is characterized by a single-ET rate constant k_2; the possibility of reverse ET is incorporated by inclusion of rate constant k_{-2}.

A key challenge in defining the mechanism of nitrogenase is to understand the steps in the kinetic scheme of eq 1 at a detailed molecular level. The process begins when the ATP-bound Fe protein with a reduced [4Fe-4S] cluster docks to the MoFe protein (Figure 1). The subsequent intracomplex ET from the Fe protein to the MoFe protein was shown to be gated in a study that employed variations in viscosities and osmotic pressures.[5] The variation of the ET rate constant with osmotic pressure showed that ∼80 waters bind to the protein surfaces during the reaction. This binding induces conformational changes in the MoFe protein that initiate "gated" electron transfer (ET)[6,7] within the MoFe protein, from the P cluster [8Fe-7S] to the FeMo cofactor.[5] This process in turn creates an electron "deficit" on the P cluster, which is backfilled by rapid electron transfer from the Fe protein to the oxidized P cluster.

Received: August 14, 2012
Revised: September 18, 2012
Published: October 10, 2012

dx.doi.org/10.1021/bi301164j | *Biochemistry* 2012, 51, 8391−8398

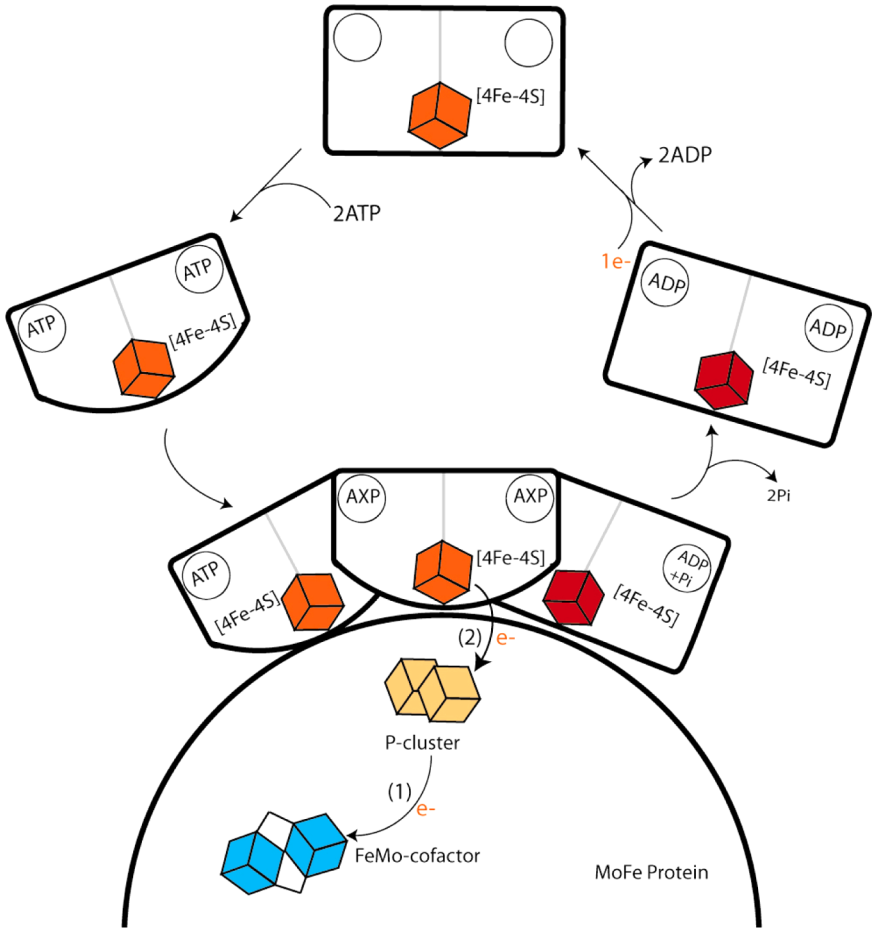

Figure 1. Events proposed to occur at the interface of the MoFe protein and the Fe protein as the latter delivers an electron to the former. Here the MoFe protein is represented by the semicircle. The Fe protein (coming in from the left) binds two molecules of ATP. The binding of ATP to the Fe protein causes conformational changes in the Fe protein that bring the [4Fe-4S] cluster closer to the surface of the protein. Conformational changes subsequent to binding "gate" the conversion to an ET-active state. As the order of ET and ADP hydrolysis is uncertain, in this state the nucleotide is written "AXP". The final step is the departure of the Fe protein (right).

X-ray crystal structures of MoFe protein−Fe protein complexes have been determined in various states of nucleotide binding.[8,9] From these structures, it is clear that the Fe protein exhibits major conformational differences in different nucleotide-bound states, and that it binds at different sites on the surface of the MoFe protein in the different states, suggesting that motion between sites is involved in the gating and inspiring the scheme implied in Figure 1. However, these structures do not show any differences within the MoFe protein, thus leaving open the nature of the motions within the MoFe protein that contribute to the gated ET.[10−12]

This ET process, which has been termed "deficit spending",[13] is linked to the hydrolysis of two ATP molecules bound to the Fe protein. Although ATP hydrolysis may well follow the ET reaction, in analogy to other NTPases,[14] the order of electron transfer and ATP hydrolysis has not been clearly established,[2,15,16] so in Figure 1, the state of the nucleotide in the ET-active conformation is not specified (X = T or D). The absence of a solvent kinetic isotope effect (sKIE)[5] at ambient temperature implied that ATP hydrolysis, which should be slowed by the presence of D versus H, is not involved in the rate-limiting step of ET.

Equation 1 is written as though the ET step is reversible. Although ET is quantitative at ambient temperature, previous studies found that the absorbance change associated with the oxidation of Fe^{red} by MoFe protein (ΔA) decreases as the temperature is lowered.[2,16] This was interpreted as indicating that ET is an equilibrium process, with an equilibrium constant at ambient temperature that is large ($K_2 = k_2/k_{-2} \gg 1$), corresponding to quantitative ET, but decreases to ~1 at 5 °C. If ET is indeed reversible, then either it precedes ATP hydrolysis or the hydrolysis also must be reversible.

A number of studies investigated the temperature dependence of ET as a means of exploring mechanism.[2,16,17] They suggested that the actual mechanism of ET from the Fe protein to the MoFe protein changes upon cooling. Thus, a nonlinear Arrhenius plot of the observed ET rate constant versus inverse temperature was interpreted as having a "break" at ~14−16 °C and used as the basis for a suggestion that one mechanism operates at higher temperatures and another at lower temperatures, each with a characteristic activation enthalpy. The proposal of a change in mechanism was supported by stopped-flow (SF) isothermal calorimetry (ITC) measurements, which were interpreted as showing that in the low-temperature regime the hydrolysis of ATP precedes the electron transfer event, whereas at ambient temperature the ET event occurs prior to ATP hydrolysis.[16]

Here, we have re-examined the temperature variations at a constant pH in the extent and rate constants for oxidation of the Fe protein by the MoFe protein within the preformed

dx.doi.org/10.1021/bi301164j | *Biochemistry* 2012, 51, 8391−8398

complex and have tested for the persistence of gating at low temperatures and the appearance of an sKIE on ET. Our findings show that the ET mechanism does not change during cooling at a constant pH.

MATERIALS AND METHODS

All reagents for these experiments were purchased from Sigma-Aldrich Chemicals (St. Louis, MO). Wild-type MoFe protein was expressed in *Azotobacter vinelandii* strain DJ995, while wild-type Fe protein was obtained from strain DJ884 grown as described previously.[18] MoFe protein was purified using the previously described metal affinity chromatography method because of the seven-histidine tag on the α-subunit of the protein, while Fe protein was purified, with some modifications, using ion exchange and size exclusion as previously described.[18,19] Both proteins utilized in these experiments were found to be >95% pure based on sodium dodecyl sulfate–polyacrylamide gel electrophoresis analysis using Coomassie blue staining. Septum-sealed degassed vials, under an argon atmosphere, were used to determine the activity of the proteins. The wild-type Fe protein activity was found to be ~1750 nmol, while the wild-type MoFe protein activity was found to be ~2100 nmol. Both activities were similar to previously reported values for the activities of these proteins.[20] All liquids were transferred using gastight syringes.

The increase in absorbance at 430 nm was monitored to follow the ET from the Fe protein to the MoFe protein. This increase in absorbance occurs due to the Fe protein's oxidation by one electron from its reduced +1 state to the +2 state; there is no significant accompanying change in the aborbance of the MoFe protein. The change in absorbance as a function of time after the mixing of the two proteins was observed using a Hi-Tech SF61 stopped-flow (SF) UV–visible spectrophotometer equipped with data acquisition software (Salisbury, Witts, U.K.). The SF unit of the spectrophotometer was housed inside a nitrogen-filled glovebox. The temperature during the experiments was controlled by a circulating water bath housed outside the glovebox.[21] All reactions, except for the change in temperature experiments, were conducted at 25 °C. Differing buffer systems, 4-(2-hydroxyethyl)-1-piperazineethanesulfonic acid (HEPES) and 3-(*N*-morpholino)propanesulfonic acid (MOPS) (pH 7.4), were used with 10 mM dithionite. Because of the change in pH with temperature in HEPES buffer, MOPS was utilized for the temperature dependency experiments to keep the pH constant.[22] During the SF experiments, Fe and MoFe protein were contained in one drive syringe of the unit while the other syringe contained $MgCl_2$ and ATP. Both syringes contained buffer [100 mM HEPES/MOPS (pH 7.4)] and 10 mM dithionite. The dead time of the Hi-Tech SF61 SF system is 2 ms.

In our experiments, the formation of the $[Fe^{red}(MgATP^*)_2;MoFe]$ complex is essentially quantitative and complete within the dead time of the experiment. Thus, the SF trace monitors the intracomplex oxidation, $Fe^{red} \rightarrow Fe^{ox}$, by MoFe protein, the second step in eq 1. In the SF experiment, the absorbance of the mixed solutions prior to $Fe^{red} \rightarrow Fe^{ox}$ oxidation is obtained with a nonreactive "push" in which ATP is omitted, and then the instrument output is "nulled" by subtraction of this absorbance. As a result, the SF traces represent the time variation of the absorbance difference caused by the reaction, relative to that of the initial mixed, unreacted solution.

Previous studies typically yielded the rate constant for the oxidation of Fe^{red}, denoted here k_{obs}, by fitting the initial portion of the SF traces with an exponential rise to maximum.[2,5,16,17] However, as one can see in the data presented below (Figure 2) and in the Supporting Information,

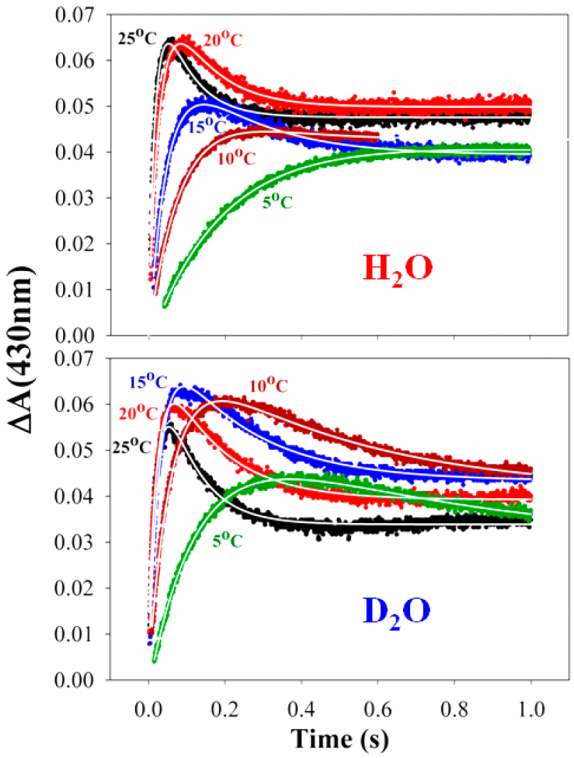

Figure 2. Temperature-response stopped-flow traces for the oxidation of Fe^{red} within the $[Fe^{red}(MgATP)_2;MoFe]$ complex in H_2O and D_2O buffers: (top) H_2O and (bottom) D_2O. Plots are labeled with the temperature from 25 to 5 °C in the respective color of the traces. White lines through each trace are fits as described in Materials and Methods.

the SF traces for the oxidation of Fe^{red} by MoFe protein in general have a more complex shape, which indicates that the oxidation of Fe^{red} is followed by a slower reaction to a state with a smaller absorbance difference. Haaker and co-workers attribute this follow-up reaction to hydrolysis of ATP. Alternatively, we suggest this may represent a partial re-reduction of the resulting Fe^{ox} to Fe^{red} that occurs as part of a complex set of reactions that involves dissociation of Fe^{ox}, re-reduction to Fe^{red}, and rebinding to MoFe.[23]

In this report, we are interested only in the rate constant and absorbance difference associated with the initial intracomplex oxidation, $Fe^{red} \rightarrow Fe^{ox}$, by MoFe protein. As shown in the Supporting Information, neither of these parameters is accurately derived with a rise to maximum fit if the follow-up phase of the SF trace is appreciable, so we have employed the simplest possible kinetic model to treat the observed traces. We find that the overall traces can be well-modeled by a kinetic scheme that includes two sequential first-order reactions (eq 2)

$$[Fe^{red};MoFe^{N}] \xrightarrow{k_{obs}} [Fe^{ox};MoFe^{red}] \xrightarrow{k_{obs}} \mathbf{C} \qquad (2)$$

the first representing the initial oxidation of Fe^{red} by MoFe protein and the second a follow-up reaction to an unspecified state, denoted **C**. This model leads to an equation for the

dx.doi.org/10.1021/bi301164j | *Biochemistry* 2012, 51, 8391–8398

resolved time course of the absorbance difference, $\Delta A(\tau)$ (eq 3):

$$\Delta A(\tau) = \Delta A_o + \Delta A_r\left[\left(\frac{k_{obs}}{k_{obs} - k_{Dr}}\right)(e^{-k_{Dr}\tau} - e^{-k_{obs}\tau})\right] + \Delta A_{Dr}\left\{1 - \left[\left(\frac{-k_{Dr}}{k_{obs} - k_{Dr}}\right)e^{-k_{obs}\tau} + \left(\frac{k_{obs}}{k_{obs} - k_{Dr}}\right)e^{-k_{Dr}\tau}\right]\right\} \quad (3)$$

where $\tau = t - t_{DT}$, with t_{DT} being the time at which mixing artifacts have subsided (dead time). In this equation, k_{obs} is the rate constant for the oxidation of Fe^{red} by MoFe protein and k_{Dr} is the rate constant for the follow-up process. This equation takes into account possible reaction during the dead time leading to an absorbance difference, ΔA_o. As a result of such a phenomenon, the total absorbance difference associated with the first-step intracomplex oxidation of Fe^{red} (eq 2), denoted here ΔA, equals the absorbance change associated with the initial oxidation step in the resolved phase of eq 3, ΔA_r, plus the absorbance change from the portion of the oxidation reaction that occurs during the dead time, ΔA_o: $\Delta A = \Delta A_o + \Delta A_r$. As incorporated into eq 3, state **C** is characterized by a net absorbance difference, ΔA_{Dr}, relative to the initial state. In Results and Analysis, we discuss only the parameters associated with the initial oxidation of Fe^{red} by MoFe protein, k_{obs} and ΔA; for completeness only, values for the parameters associated with the unspecified follow-up process, k_{Dr} and ΔA_{Dr}, are given in the Supporting Information.

As discussed in detail in the Supporting Information, the fits to eq 3 give as much as a 2-fold smaller rate constant, k_{obs}, than a rise to maximum fit. However, we note that trends such as changes with temperature or osmotic pressure, which are the focus of this work, are comparably represented by the two approaches (Figure S1 of the Supporting Information).

RESULTS AND ANALYSIS

Influence of Temperature and Solvent Isotope on ET. Figure 2 shows the SF traces at different temperatures for the oxidation of Fe^{red} by the MoFe protein in H_2O (top) and D_2O (bottom) solutions with MOPS as the buffer. As this buffer has a negligible temperature coefficient pK_a versus T,[22] these measurements thus were taken with an essentially invariant pH (pD) of 7.4 over the temperature range of 5–25 °C. As discussed in Materials and Methods, above 5 °C the absorbance changes associated with the initial oxidation of Fe^{red} by MoFe do not show a simple rise to maximum; the initial absorbance increase is followed by a decrease in absorbance associated with re-reduction of Fe^{red} or the change in absorbance of Fe^{ox} due to hydrolysis of ATP. To obtain the rate constants for the initial Fe^{red} oxidation, the traces were fit to a sequential model in which the oxidation of Fe^{red} is followed by a slower re-reduction process, as described in Materials and Methods. In discussing these results, we consider only the rate constants and absorbance changes associated with the initial Fe^{red} oxidation.

To test for congruence between our results and those reported previously, the traces of Figure 2 were truncated and fit to a rise to maximum. As mentioned in Materials and Methods and shown in the Supporting Information, such fits typically give larger values for k_{obs}, in keeping with those reported previously,[2,16,17] but the trends with temperature are completely equivalent (Figure S1 of the Supporting Information). Thus, trends reported in this study can be appropriately compared to those in earlier reports. However, we believe that the magnitudes of k_{obs} based on fits to eq 3, which are notably lower than previous values, are more appropriate.

The temperature responses of the rate constants and absorbance changes associated with the initial Fe^{red} oxidation for D_2O and H_2O solutions [MOPS (pH or pD 7.4)], denoted k_{obs} and ΔA, respectively, are plotted in Figures 3 and 4,

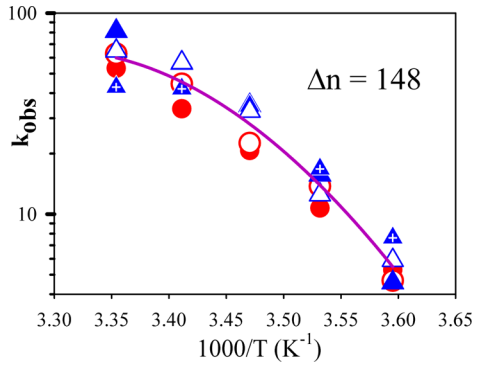

Figure 3. Semilogarithmic plot of the observed rate constants, k_{obs}, for D_2O (blue) and H_2O (red). Individual experiments are visualized by empty, filled, or crossed points. The purple solid line is a fit to all data sets, assuming that there is no difference in k_{obs} for H_2O and D_2O buffers.

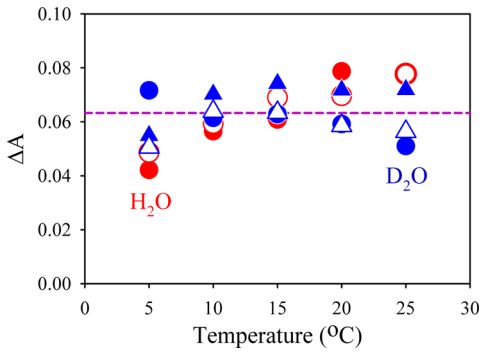

Figure 4. Temperature dependence of absorbance change ΔA (eq 3) obtained from intracomplex oxidation of $Fe^{red}(ATP)_2$ by MoFe as a function of temperature. The purple dashed line shows the averages of all values.

respectively. The observed ET rate constants decrease strongly with temperature (Figure 3), and the k_{obs} values for H_2O and D_2O solutions with MOPS are the same within experimental error. The finding that $k_{obs}(H_2O) = k_{obs}(D_2O)$ at ambient temperature confirms our earlier report that there is no sKIE at 25 °C; the equivalence of the rate constants at all temperature shows that an sKIE does not emerge upon cooling.

Temperature-Dependent ET Equilibrium? Thorneley et al. reported that the absorbance change (ΔA) associated with $Fe^{red} \rightarrow$ MoFe ET in H_2O buffer diminishes with decreasing temperature,[2] a finding corroborated by Mensink and Haaker.[16] The absorbance decrease was interpreted in terms of a temperature dependence of an ET equilibrium between the two proteins, as represented by the second step of eq 1. It was proposed that ET was essentially quantitative at 25 °C [$k_2 \gg$

dx.doi.org/10.1021/bi301164j | Biochemistry 2012, 51, 8391–8398

k_{-2} (eq 1)], but by 5 °C, only ~50% of the complexes showed ET ($k_2 \approx k_{-2}$).

There are multiple reasons for concern about these conclusions. First, the experiments were conducted with solutions that used TES/NaOH buffer and as a result were not performed at a constant pH as the temperature was lowered. TES buffers have a large temperature coefficient,[22] causing an increase in pH from 7.4 to ~7.7 as the temperature is lowered from 25 to 5 °C. Second, the kinetic traces were fit to a simple rise to maximum function, which does not necessarily give a good representation of the maximal absorbance change when the reaction involves more than one stage (eq 1). In particular, as has been reported, the kinetic traces often show a rise to maximum, a slight fall, and then a slow rise.[2]

We thus analyzed the temperature dependence of the absorbance changes associated with the ET kinetic measurements discussed above. Figure 4 shows that these absorbance changes fluctuate appreciably from one experiment to the next, even though the kinetic constants do not (Figure 3). However, within the error of our measurements, the absorbance changes with MOPS as the buffer are the same for H_2O and D_2O solutions and are invariant with temperature; the same is true for the absorbance changes obtained from rise to maximum fits (Figure S2 of the Supporting Information). We tested whether the implied constancy in the extent of ET is modified by a change with cooling of the difference between the extinction coefficients of oxidized and reduced Fe protein [$\Delta\varepsilon = \varepsilon(Fe^{ox}) - \varepsilon(Fe^{red})$]. As shown in Figure S3 of the Supporting Information, within error, this difference is temperature invariant down to 5 °C. We thus interpret the results of Figure 4 as showing that the quantitative ET in MOPS buffer at pH 7.4 is essentially unchanged during cooling at a constant pH from 25 to 5 °C. In the description of nitrogenase ET given by eq 1, the observed ET rate constant is related to the microscopic rate constants by $k_{obs} = k_2 + k_{-2}$. However, when ET is quantitative, the ET rate constants obey the inequality $k_2 \gg k_{-2}$, and thus, we may assign $k_{obs} = k_2$ throughout the temperature range examined.

To test whether the previously reported temperature response of ΔA associated with $Fe^{red} \rightarrow$ MoFe ET in H_2O buffer could be attributed to a change in pH upon cooling, the temperature dependence of ET was re-examined using samples prepared with HEPES/H_2O buffer (Figure S4 of the Supporting Information). HEPES has a temperature coefficient similar to that of TES, used by Haaker and co-workers; with HEPES as the buffer, the pH increases from 7.4 to ~7.8 as the temperature is lowered from 25 to 5 °C. As shown in Figure S5 of the Supporting Information, the absorbance change associated with $Fe^{red} \rightarrow$ MoFe protein ET for H_2O solutions of HEPES buffer indeed decreases by roughly 50% from 25 to 5 °C, whereas the absorbance change does not decrease for the D_2O solutions of HEPES buffer (Figure S4 of the Supporting Information) and, if anything, increases slightly with a decrease in temperature. The differing behaviors for the H_2O and D_2O solutions with HEPES presumably reflect an equilibrium isotope effect on the pH dependence of the extent of ET. This inference is supported by measurements over a range of pH values in HEPES buffer, all taken at 5 °C (Figures S6 and S7 of the Supporting Information). These show that k_{obs} does not change significantly with pH for either buffer; there is a substantial variation in ΔA with pH for the H_2O buffers but a negligible change for the D_2O buffers.

Gating at Low Temperatures? To reveal if conformational gating of ET from the Fe protein to the MoFe protein persists at temperatures below the apparent break temperature (T_b ~ 14−16 °C) as concluded in earlier studies, we examined the influence of osmolytes on k_{obs} for ET at 6 °C. Sucrose, glycerol, and glucose were studied as osmolytes because they generated the strongest, intermediate, and weakest effects, respectively, seen at ambient temperature.[5] As illustrated for sucrose as the solute in Figure 5 (inset), progressive additions

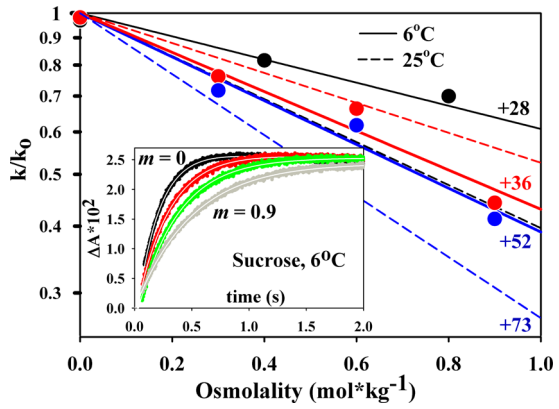

Figure 5. Plot of the solute-dependent osmotic effect on nitrogenase: black for glycerol, red for glucose, and blue for sucrose. Points and solid lines represent results at 6 °C; dashed lines represent the previously published results at 25 °C. Glycerol alone could be examined to higher m values, and the additional points are shown in Figure S1 of the Supporting Information. The inset shows the stopped-flow oxidation of Fe^{red} within the [$Fe^{red}(MgATP)^2$:MoFe] complex with increasing amounts of sucrose.

of each osmolyte cause progressive decreases in k_{obs} at 6 °C, thus indicating that ET is under conformational control at this low temperature as well as at ambient temperature. Given the observed control of ET by osmotic pressure effects at 6 and 25 °C, we conclude that the gating mechanism that controls ET persists throughout the temperature range.

Changes in osmotic pressure modulate the energetics of reactions that change the number of bound waters. The rate constant for such a process varies exponentially with the molality of added solute (m) according to the equation[24] $k(m) \propto \exp[-(\Delta n/55.6)m]$, where Δn is the number of waters absorbed in the transformation. Logarithmic plots of k_{obs} at 6 °C versus the molality for each solute employed are linear, as they are at ambient temperature (Figure 5), revealing that the osmotic pressure effects that control ET at ambient temperature persist at reduced temperatures. This linearity persists to higher osmolalities, as shown in Figure S8 of the Supporting Information. The slopes of these lines, which differ for the different osmolyes, reflect the numbers of waters absorbed during ET: slope = $-(\Delta n/55.6)$. At 25 °C, Δn = 50−80 for the three osmolytes; at 5 °C, Δn = 30−50. The decreased values of Δn at 6 °C suggest that the osmolytes interact more strongly with the surface as the temperature is decreased.

The absence of an H_2O versus D_2O solvent kinetic isotope effect (sKIE) for ET between the Fe protein and the MoFe protein at 6 °C indicates that ATP hydrolysis is not rate-limiting at low temperatures, just as it is not rate-limiting at 25 °C. In combination with the unchanging osmotic pressure effects over the temperature range, the results indicate that the order of the ATP hydrolysis event is unaffected by the change

dx.doi.org/10.1021/bi301164j | Biochemistry 2012, 51, 8391−8398

in temperature and are consistent with there being no change in the mechanism with a change in temperature. This conclusion is contrary to the earlier ITC findings that ATP hydrolysis precedes electron transfer at lower temperatures.

Does the Temperature Variation of k_{obs} Imply a Change in Mechanism? The Arrhenius plots of $\ln(k_{obs})$ versus $1/T$ presented in Figure 3 for both H_2O and D_2O MOPS solutions are nonlinear, consistent with earlier findings for experiments conducted with H_2O buffer solutions.[2,17] The earlier work interpreted this nonlinearity to indicate a change in ET mechanism as the temperature is lowered from ambient temperature. Those temperature variations were analyzed in terms of an apparent break at $T_b \sim 14-16$ °C that separates two linear segments in the plots of $\ln(k_{obs})$ versus $1/T$. Each segment was fit to its own slope, $(-\Delta H^{\ddagger}/R)$; each temperature range was assigned a different mechanism with a characteristic enthalpy of activation, $\Delta H^{\ddagger}$, that is constant over the range. However, a real break in slope is not possible for a finite system.[25] Instead, our finding that waters become bound to the protein−protein complex during the ET process requires that the Arrhenius plot be curved, even though the mechanism does not change. The binding of Δn waters during the ET reaction causes a change in the heat capacity, ΔC_p, which one can approximate with the relationship $\Delta C_p \sim \Delta n[C_{pm}(\text{ice}) - C_{pm}(\text{liquid})] \sim \Delta n(-37\ \text{J K}^{-1}\ \text{mol}^{-1})$. This heat capacity difference in turn makes the enthalpy change associated with the ET event temperature-dependent, which induces curvature into the Arrhenius plot.

Taking the ET reaction as being governed by a conformational gating process that involves water binding,[5] we now show that the temperature variation of the ET rate constant ($k_{obs} = k_2$) can be described with a single set of thermodynamic parameters over the entire range of temperatures examined. Taking as a reference temperature that of the apparent break, T_b, one can write the enthalpy change for the ET reaction at any temperature within this range as the sum of a termperature-independent enthalpy change, $\Delta H(T_b)$, plus the temperature-dependent contribution associated with water binding[26]

$$\Delta H(T) = \Delta H(T_b) + \Delta C_p(T - T_b) \tag{4}$$

A Gibbs−Helmholtz equation for k_{obs} then leads to a temperature dependence, eq 5. [26]

$$\ln\left[\frac{k_{obs}(T)}{k_{obs}(T_b)}\right] = -\frac{\Delta H(T_b)}{R}\left(\frac{1}{T} - \frac{1}{T_b}\right) + \frac{\Delta C_p}{R}\left[\ln\left(\frac{T}{T_b}\right) + \frac{T_b}{T} - 1\right] \tag{5}$$

As shown in Figure 3, the combined temperature responses of k_{obs} in H_2O and D_2O buffers are indeed described well by the continuous function (eq 5) with a single set of enthalpic parameters, $\Delta H(T_b)$ and ΔC_p, and thus by a single mechanism.

The resulting constant contribution to the enthalpy change $[\Delta H(T_b) = 130\ \text{kJ/mol}]$ of eq 5 is roughly the average of the values that would be obtained from a partition of the experimental data into two linear segments, with separate fits for each segment. The ΔC_p value of $-5.5\ \text{kJ mol}^{-1}\ \text{K}^{-1}$ corresponds to the uptake of ∼150 waters (Δn). Although Δn is considerably larger than the Δn determined in the osmotic pressure measurements, given that the latter suggest that Δn may change with T and the simplified form of eq 4, we take the osmotic pressure measurements and temperature dependence of the ET rate constants as being satisfactorily self-consistent.

DISCUSSION

We have examined the temperature variation in the kinetics of oxidation of the Fe protein by the MoFe protein and tested for osmotic pressure effects and sKIE. The findings can be summarized as follows. (i) As the temperature is lowered from 25 to 5 °C at a constant pH fixed by MOPS buffer, the observed rate constant for Fe^{red} → MoFe protein ET decreases strongly, but with a nonlinear Arrhenius plot, consistent with previous reports that employed buffers with high temperature coefficients. (ii) ET remains gated at the lowest temperature by a conformational change that involves the binding of numerous water molecules, and cooling does not introduce an sKIE. (iii) These observations contradict the earlier proposals of a change in ET mechanism with cooling. (iv) In support of this mechanistic invariance, it is shown that the nonlinear Arrhenius plot for the ET rate constant arises from the change in heat capacity associated with the binding of waters and does not indicate a change in mechanism. (v) Finally, it is shown that the extent of Fe protein to MoFe protein ET at a constant pH does not change substantially with temperature, in contrast to the changing ET equilibrium inferred previously from experiments in which cooling was accompanied by an increase in pH. Overall, these findings address multiple issues associated with intercomponent oxidation of Fe^{red} by MoFe and overturn some long-held views about this process.

Our earlier study of intracomplex ET at ambient temperature employed the addition of viscogen/osmolyte solutes to reveal that the process is gated and responds to osmotic pressure effects, not changes in viscosity.[5] The changes in k_{obs} with osmolality were interpreted as reflecting the binding of ∼50−80 waters (Δn) during ET, and it was inferred that this is associated with motions at the Fe−MoFe protein interface. We here show that osmotically controlled gating persists to 5 °C. The osmolality dependence of k_{obs} at 5 °C indicates that somewhat fewer waters bind upon cooling ($\Delta n = 30-50$), a result that may be attributed to an increased level of interaction of osmolytes with protein surfaces at the lower temperatures.

The finding that ET remains gated down to the lowest temperature examined, along with the finding that ET is independent of solvent isotopic composition over the entire temperature range, suggests that the ET mechanism does not change upon cooling. Moreover, the observed osmotic pressure dependence provides the foundation for the explanation of the nonlinear Arrhenius plots of k_{obs} in terms of a single, unchanging mechanism. The proposed analysis in terms of two linear segments that intersect at a break temperature of 15 °C that separates two temperature regions in which different mechanisms operate[16,17] is thermodynamically untenable, while the finding that waters become bound during ET requires that the Arrhenius plot be nonlinear even without a change in mechanism. When waters bind during the reaction, the enthalpy of activation, $\Delta H^{\ddagger}$, becomes temperature-dependent because the heat capacity is different for free and bound waters (eq 4). Application of a Gibbs−Helmholtz equation to the ET rate constant then necessarily yields a nonlinear Arrhenius plot (eq 4). As shown in Figure 3, the temperature response of k_{obs} can be described well by a fit to eq 5, with a plausible value for the number of waters bound during ET. This eliminates the basis of the earlier suggestions for a change in mechanism.

dx.doi.org/10.1021/bi301164j | Biochemistry 2012, 51, 8391−8398

This report further gives an alternative explanation to earlier reports that the extent of ET decreases from ~100% at ambient temperature to ~50% as the temperature decreases to ~5 °C. Experiments conducted with MOPS, a buffer whose pK_a changes negligibly with temperature, indicate that at a constant pH the extent of ET does not change within error upon cooling from 25 to 5 °C, and that this invariance is independent of solvent isotope (H or D). Thus, our measurements indicate that the extent of ET at constant pH is not temperature-dependent.

We do corroborate the finding that the extent of ET does change upon cooling of solutions prepared with buffers with a large temperature coefficient (HEPES buffer in our experiments and TES buffer in previous work). The pH changes by roughly 0.5 unit when these buffer solutions are cooled to 5 °C, and thus, the changes in behavior upon cooling can be assigned not to the temperature variation of ET but to a pH dependence of the extent of ET at 5 °C, which has been observed explicitly (Supporting Information). A determination of the origin of this dependence is beyond the scope of this report.

CONCLUSIONS

The deficit spending mechanism for $Fe^{red} \rightarrow$ MoFe protein ET that operates at ambient temperature does not change upon cooling to 5 °C at a constant pH. This mechanism likely is associated in some part with motions at the interface between the two proteins of the type depicted in Figure 1. The change in heat capacity caused by binding of waters during the ET process leads to a nonlinear Arrhenius plot of the rate constant for ET versus inverse temperature, invalidating earlier interpretations of this nonlinearity in terms of a change in ET mechanism. The extent of ET observed at ambient temperature does not change during cooling at constant pH but likely varies with pH at a constant low temperature, where it also depends on solvent isotope. The origin of this last effect, suggestive of an equilibrium solvent isotope effect, remains to be determined.

ASSOCIATED CONTENT

Supporting Information

Ten figures that present additional experimental data and one chart that addrsses procedures for analysis. This material is available free of charge via the Internet at http://pubs.acs.org.

AUTHOR INFORMATION

Corresponding Author

*L.C.S.: e-mail, lance.seefeldt@usu.edu; phone, (435) 797-3964; fax, (435) 797-3390. B.M.H.: e-mail, bmh@northwestern.edu; phone, (847) 491-3104; fax, (847) 491-7713.

Funding

This work has been supported by the National Institutes of Health (Grant HL 13531 to B.M.H. and Grant GM 59087 to D.R.D. and L.C.S.).

Notes

The authors declare no competing financial interest.

ABBREVIATIONS

ET, electron transfer; sKIE, solvent kinetic isotope effect; SF, stopped-flow.

REFERENCES

(1) Smil, V. (2001) *Enriching the Earth: Fritz Haber, Carl Bosch, and the Transformation of World Food Production*, MIT Press, Cambridge, MA.

(2) Thorneley, R. N. F., Ashby, G., Howarth, J. V., Millar, N. C., and Gutfreund, H. (1989) A transient-kinetic study of the nitrogenase of *Klebsiella pneumoniae* by stopped-flow calorimetry. Comparison with the myosin ATPase. *Biochem. J. 264*, 657−661.

(3) Burgess, B. K., and Lowe, D. J. (1996) Mechanism of molybdenum nitrogenase. *Chem. Rev. 96*, 2983−3011.

(4) Wilson, P. E., Nyborg, A. C., and Watt, G. D. (2001) Duplication and extension of the Thorneley and Lowe kinetic model for *Klebsiella pneumoniae* nitrogenase catalysis using a MATHEMATICA software platform. *Biophys. Chem. 91*, 281−304.

(5) Danyal, K., Mayweather, D., Dean, D. R., Seefeldt, L. C., and Hoffman, B. M. (2010) Conformational gating of electron transfer from the nitrogenase Fe protein to MoFe protein. *J. Am. Chem. Soc. 132*, 6894−6895.

(6) Hoffman, B. M., and Ratner, M. R. (1987) Gated electron transfer: When are observed rates controlled by conformational interconversion? *J. Am. Chem. Soc. 109*, 6237−6243.

(7) Hoffman, B. M., Ratner, M. A., and Wallin, S. A. (1990) Energetics and dynamics of gated reactions: Control of observed rates by conformational interconversion. In *Advances in Chemistry* (Johnson, M. K., King, R. B., Kurtz, D. M., Jr., Kutal, C., Norton, M. L., and Scott, R. A., Eds.) pp 125−146, American Chemical Society, Washington, DC.

(8) Tezcan, F. A., Kaiser, J. T., Mustafi, D., Walton, M. Y., Howard, J. B., and Rees, D. C. (2005) Nitrogenase complexes: Multiple docking sites for a nucleotide switch protein. *Science 309*, 1377−1380.

(9) Rees, D. C., Tezcan, F. A., Haynes, C. A., Walton, M. Y., Andrade, S., Einsle, O., and Howard, J. B. (2005) Structural basis of biological nitrogen fixation. *Philos. Trans. R. Soc. London, Ser. A 363*, 971−984.

(10) Although binding of water at an interface can enhance ET (refs 11 and 12) and thus may contribute to gating, we surmise it is the unknown motions within the MoFe protein that are most important here.

(11) de la Lande, A., Babcock, N. S., Rezac, J., Sanders, B. C., and Salahub, D. R. (2010) Surface residues dynamically organize water bridges to enhance electron transfer between proteins. *Proc. Natl. Acad. Sci. U.S.A. 107*, 11799−11804.

(12) Keinan, S., Nocek, J. M., Hoffman, B. M., and Beratan, D. N. (2012) Interfacial hydration, dynamics and electron transfer: Multiscale ET modeling of the transient [Myoglobin, Cytochrome b5] complex. *Phys. Chem. Chem. Phys. 14*, 13881−13889.

(13) Danyal, K., Dean, D. R., Hoffman, B. M., and Seefeldt, L. C. (2011) Electron transfer within nitrogenase: Evidence for a deficit-spending mechanism. *Biochemistry 50*, 9255−9263.

(14) Altenberg, G. A. (2004) Structure of multidrug-resistance proteins of the ATP-binding cassette (ABC) superfamily. *Curr. Med. Chem.: Anti-Cancer Agents 4*, 53−62.

(15) Lowe, D. J., Ashby, G. A., Brune, M., Knights, H., Webb, M. R., and Thorneley, R. N. F. (1995) ATP hydrolysis and energy transduction by nitrogenase. In *Nitrogen Fixation: Fundamentals and Applications* (Tikhonovich, I. A., Provorov, N. A., Romanov, V. I., and Newton, W. E., Eds.) pp 103−108, Kluwer Academic Publishers, Dordrecht, The Netherlands.

(16) Mensink, R. E., and Haaker, H. (1992) Temperature effects on the magnesium-ATP-induced electron transfer between the nitrogenase proteins from *Azotobacter vinelandii*. *Eur. J. Biochem. 208*, 295−299.

(17) Lanzilotta, W. N., Parker, V. D., and Seefeldt, L. C. (1998) Electron transfer in nitrogenase analyzed by Marcus theory: Evidence for gating by MgATP. *Biochemistry 37*, 399−407.

(18) Christiansen, J., Goodwin, P. J., Lanzilotta, W. N., Seefeldt, L. C., and Dean, D. R. (1998) Catalytic and biophysical properties of a nitrogenase apo-MoFe protein produced by a nifB-deletion mutant of *Azotobacter vinelandii*. *Biochemistry 37*, 12611−12623.

(19) Burgess, B. K., Jacobs, D. B., and Stiefel, E. I. (1980) Large-scale purification of high activity *Azotobacter vinelandii* nitrogenase. *Biochim. Biophys. Acta 614*, 196−209.
(20) Seefeldt, L. C., Morgan, T. V., Dean, D. R., and Mortenson, L. E. (1992) Mapping the site(s) of MgATP and MgADP interaction with the nitrogenase of *Azotobacter vinelandii*. Lysine 15 of the iron protein plays a major role in MgATP interaction. *J. Biol. Chem. 267*, 6680−6688.
(21) Lanzilotta, W. N., Fisher, K., and Seefeldt, L. C. (1996) Evidence for electron transfer from the nitrogenase iron protein to the molybdenum−iron protein without MgATP hydrolysis: Characterization of a tight protein−protein complex. *Biochemistry 35*, 7188−7196.
(22) Good, N. E., Winget, G. D., Winter, W., Connolly, T. N., Izawa, S., and Singh, R. M. M. (1966) Hydrogen ion buffers for biological research. *Biochemistry 5*, 467−477.
(23) Thorneley, R. N. F., and Lowe, D. J. (1985) Kinetics and mechanism of the nitrogenase enzyme system. In *Molybdenum Enzymes* (Spiro, T. G., Ed.) pp 89−116, Wiley-Interscience, New York.
(24) Parsegian, V. A., Rand, R. P., and Rau, D. C. (1995) Macromolecules and water: Probing with osmotic stress. *Methods Enzymol. 259*, 43−94.
(25) An abrupt break in a plot such as that in Figure 4 would imply the existence of a second-order phase change and could not actually occur in a molecular system.
(26) If the ET rate constant corresponds to that for the conformational gate, then its temperature response is characterized by the activation enthalpy. If ET involves a conformational preequilibrium, then the temperature variation would be described by the sum of the enthalpy change for the gating equilibrium and the ET activation enthalpy. In either case, in a precise application of transition-state theory, the $k_{obs}(T)/k_{obs}(T_b)$ ratio would be replaced by $T_b[k_{obs}(T)]/T[k_{obs}(T)]$, but over the narrow range of temperatures examined, the parameters derived from such a fit differ insignificantly from that to the more intuitive eq 5.